Curr Pharmacol Rep (2016) 2:193–201
DOI 10.1007/s40495-016-0063-0

CHEMICAL AND MOLECULAR TOXICOLOGY (J BOLTON, SECTION EDITOR)

A Critical Review of Methodologies to Detect Reactive Oxygen and Nitrogen Species Stimulated by NADPH Oxidase Enzymes: Implications in Pesticide Toxicity

Balaraman Kalyanaraman[1] · **Micael Hardy**[2] · **Jacek Zielonka**[1]

Published online: 12 May 2016

Abstract In this review, potential fluorescent probe applications for detecting reactive oxygen and nitrogen species (ROS/RNS) generated from NADPH oxidases (e.g., Nox2) and nitric oxide synthase enzymes are discussed in the context of pesticide toxicology. Identification of the specific marker products derived from the interaction between ROS/RNS and the fluorescent probes (e.g., hydroethidine and coumarin boronate) is critical. Due to the complex nature of reactions between the probes and ROS/RNS, we suggest avoiding the use of fluorescence microscopy for detecting oxidizing/nitrating species. We also critically examined the viability of using radiolabeling or positron emission tomography (PET) for ROS/RNS detection. Although these techniques differ in sensitivity and detection modalities, the chemical mechanism governing the reaction between these probes and ROS/RNS should remain the same. To unequivocally detect superoxide with these probes (i.e., radiolabeled and PET-labeled hydroethidine analogs), the products should be isolated and characterized by LC-MS/MS or HPLC using an appropriate standard.

This article is part of the Topical Collection on *Chemical and Molecular Toxicology*

✉ Balaraman Kalyanaraman
balarama@mcw.edu

[1] Department of Biophysics and Free Radical Research Center, Medical College of Wisconsin, 8701 Watertown Plank Road, Milwaukee, WI 53226, USA

[2] Aix Marseille Université, CNRS, ICR UMR 7273, 13397 Marseille, France

Keywords NADPH oxidase · Pesticides · ROS · Fluorescence probes · Superoxide · Hydrogen peroxide · Peroxynitrite

Introduction

Epidemiological studies support the notion that chronic exposure to organochlorine and related pesticides that are resistant to metabolism increases the risk factor for developing inflammatory cardiovascular and neurodegenerative diseases and cancer [22]. Although the actual mechanism responsible for the toxicity of organic pesticides is not completely understood, increased systemic oxidative stress triggered by elevated levels of reactive oxygen and nitrogen species (ROS/RNS) reportedly plays a key role [19]. The two major sources of ROS proposed to be responsible for the toxicity observed are mitochondria and NADPH oxidase enzymes (Nox) [9]. In this article, we focus mainly on Nox enzymes, especially Nox2, due to their role in the molecular mechanisms of pesticide toxicity [18].

ROS/RNS Cascade in Inflammatory Microenvironment

Figure 1 summarizes the cascade of oxidizing and nitrating species triggered by chlorinated-pesticide-induced generation of the superoxide radical anion ($O_2^{\cdot-}$). $O_2^{\cdot-}$, which is predominantly released upon Nox activation, can dismutate to form hydrogen peroxide (H_2O_2) or react with nitric oxide ($^{\bullet}NO$) at a diffusion-controlled rate to form peroxynitrite ($ONOO^-$) [3, 28]. In the presence of bicarbonate (HCO_3^-), which is ubiquitously present in cells, $ONOO^-$ forms another transient intermediate, nitrosoperoxycarbonate ($ONOOCO_2^-$), that

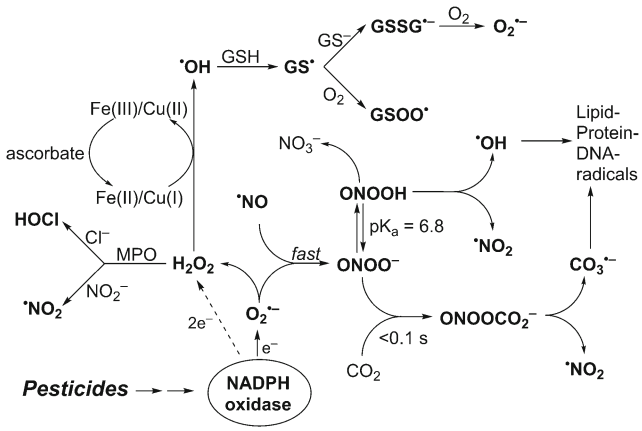

Fig. 1 ROS/RNS-induced radical cascade induced by superoxide and nitric oxide

decomposes to form nitrogen dioxide ($^{\bullet}NO_2$) and the carbonate radical anion ($CO_3^{\bullet-}$), another highly potent one-electron oxidizing species. In addition, the formation of a chlorinating oxidant, hypochlorous acid (HOCl) from myeloperoxidase (MPO)/H_2O_2/chloride anion (Cl^-) oxidation, and hydroxyl radical ($^{\bullet}OH$) from the redox-metal ion (e.g., reduced iron or copper) catalyzed reduction of H_2O_2 is also likely. MPO may also catalyze oxidation of the nitrite anion by H_2O_2 to produce nitrogen dioxide, $^{\bullet}NO_2$. Generation of other radicals derived from glutathione (GSH) such as the glutathiyl radical ($GS^{\bullet}$) and their reaction with oxygen to form oxidizing radicals ($GSOO^{\bullet}$) is also a distinct possibility. Because of this ROS/RNS cascade in the intracellular milieu, detection and assessment of the roles of different species using a single or several redox probes are nearly impossible without understanding their redox chemistry (reaction kinetics and product analyses) [47, 49]. Lack of progress in this area has so far stymied our understanding of Nox involvement in many areas of research, including pesticide toxicology.

Organochlorine Pesticides and NADPH Oxidase Activation

Organic chlorinated compounds (e.g., dieldrin, a metabolite of dichlorodiphenyltrichloroethane [DDT], dichlorodiphenyldichloroethylene [DDE], polychlorinated biphenyls [PCBs]) are mostly resistant to metabolism and biodegradation. Consequently, these chemicals tend to bioaccumulate in fatty tissues and release slowly with time, causing oxidative stress. Recent reports suggest that these chemicals activate Nox complex through activation of phospholipases A_2/arachidonic acid (PLA_2/AA) in monocyte/macrophages [18]. Monocytes treated with organochlorinated compounds enhanced Nox assembly and activation [18].

Unlike other redox-active enzymes in mitochondria and cytosolic compartments from which generation of ROS is an "accidental" byproduct of their primary catalytic function, the only known function of Nox enzymes is generation of $O_2^{\cdot-}$ and H_2O_2 [15, 24]. Several Nox isoforms including Nox2 form both $O_2^{\cdot-}$ and H_2O_2 (via dismutation of $O_2^{\cdot-}$), with the exception of Nox4 that generates primarily H_2O_2 with little or no detectable $O_2^{\cdot-}$ [24, 30, 51]. High levels of $O_2^{\cdot-}$ generated from Nox2 are essential for bacterial cell killing and host defense, and low levels of ROS are chronically generated from Nox2 in response to stimulation (e.g., phorbol myristate ester [PMA]). PMA activates protein kinase C, leading to the phosphorylation of the p47*phox* cytosolic subunit, which in turn binds to the p22*phox* membrane protein [14]. After the assembly of all cytosolic and membrane components, NADPH is oxidized and electrons are transferred to oxygen, forming $O_2^{\cdot-}$. Exogenously added compounds can activate or inhibit Nox expression, ligand receptor binding, trafficking of Nox components to cell membrane, activation and assembly of Nox complex, and/or affect NADPH binding, and electron transfer from the active site of the enzyme [2].

Recent studies have shown that organochlorine insecticides (*trans*-nonachlor, dieldrin, and DDE) induced enhanced expression of phospho-p47*phox* and enhanced its membrane localization [18]. Mechanistically, this was attributed to (PLA_2) activation, leading to increased arachidonic acid and eicosanoid production in monocytes treated with organochlorinated compounds [18]. Chronic activation of monocytes by environmental toxicants could induce Nox activation through enhanced phosphorylation of p47*phox* mediated by protein kinase C activation and arachidonic acid release and subsequent translocation of p47*phox* to cell membranes [18]. Other xenobiotics such as dieldrin, lindane, paraquat, and rotenone activate microglial Nox, stimulating Nox-dependent ROS formation. Chemicals like 1-methyl-4-phenyl-1,2,3,6-tetrahydropyridine (MPTP) induce Nox2 expression and oxidative and nitrative stress in the substantia nigra of mice [8]. The oxidative metabolite 1-methyl-4-phenylpyridinium cation (MPP^+) was shown to be the ultimate toxic metabolite. Activation of Nox2 and inducible nitric oxide synthase (iNOS) in glial cells is thought to be a major mechanism of toxicity. Reports suggest that organochlorine pesticides increase intracellular superoxide levels through activation of the PLA_2/AA/Nox signaling, thereby posing a major risk factor for the onset of metabolic and cardiovascular diseases [18].

Probes for Superoxide Detection

More than a decade ago, we showed that hydroethidine (HE) or dihydroethidium (DHE) reacts with $O_2^{\cdot-}$ to form exclusively a highly diagnostic marker product, 2-hydroxyethidium (2-OH-E^+) ([41, 42]; Fig. 2; Table 1). This finding negated the previous notion that ethidium (E^+) is the product of oxidation

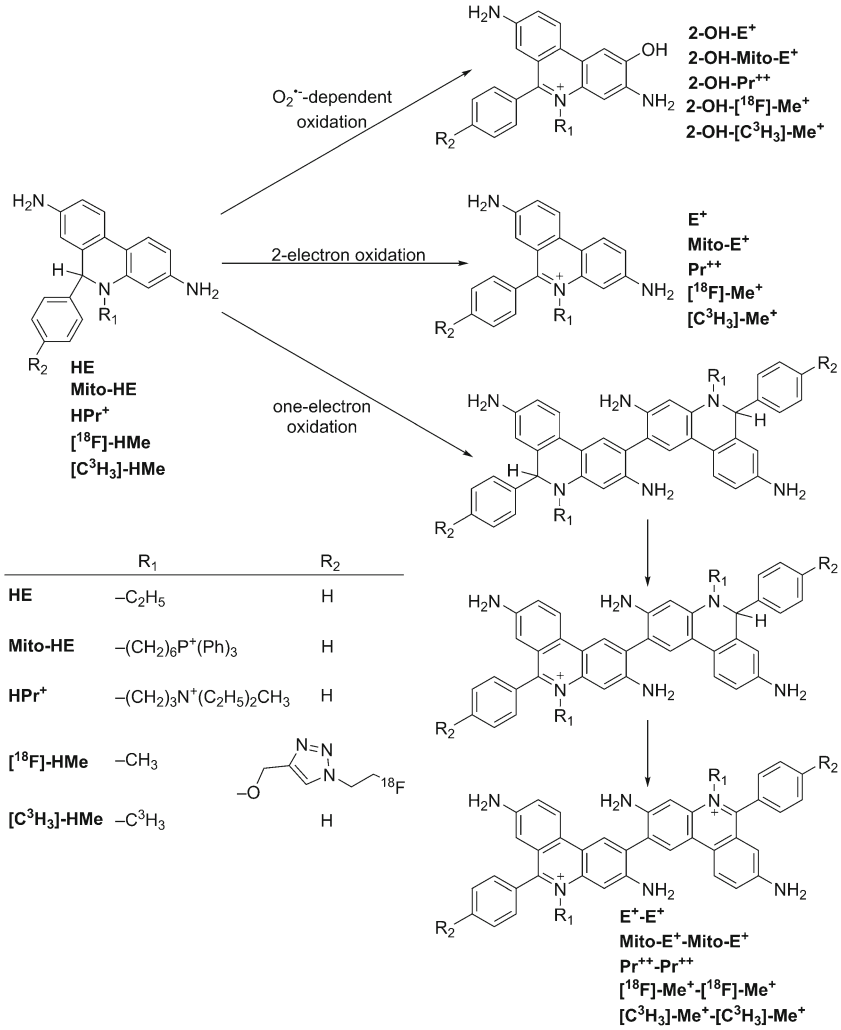

Fig. 2 Chemical structures and oxidant-dependence of the products formed from hydroethidine (HE), MitoSOX Red (Mito-HE), hydropropidine (HPr^+), ^{18}F-labeled hydromethidine ([^{18}F]-HMe), and tritium (^{3}H)-labeled hydromethidine ([C^3H_3]-HMe) probes

of HE by $O_2^{\cdot-}$ [5]. We also showed that both 2-OH-E^+ and E^+ have very similar fluorescence characteristics, and thus, fluorescence microscopy is not a viable and reliable option to monitor intracellular $O_2^{\cdot-}$ formation [42, 45]. However, HPLC or ultra-high-performance liquid chromatography (UHPLC) and liquid chromatography-mass spectrometry (LC-MS/MS) approaches were used to separate and quantify 2-OH-E^+ [45, 51]. Extensive research on the oxidation chemistry of HE revealed formation of both one- and two-electron oxidation products [46]. These include ethidium and several dimeric products that are all detectable by UHPLC [12, 51]. An additional benefit from HPLC (or LC-MS)-based detection and quantification of different HE oxidation products is the ability to monitor HOCl formation by following the formation of 2-chloroethidium (2-Cl-E^+, Table 1), in case of H_2O_2/MPO/Cl^- system [10]. In contrast to other redox-sensitive fluorophores (e.g., dichlorodihydrofluorescein [DCFH], dihydrorhodamine [DHR]), and chemiluminescent probes (lucigenin, luminol, L-012)—which form radicals that react with oxygen to form superoxide—the HE-derived radical does not react with oxygen to form superoxide [47].

Another related cell-impermeable analog of HE is hydropropidine (HPr^+), formed from a two-electron reduction of propidium (Pr^{++}) ([20]; Fig. 2; Table 1). We showed that the oxidation chemistry of HPr^+ is very similar to that of HE. Briefly, the $HPr^+/O_2^{\cdot-}$ reaction formed 2-hydroxypropidium (2-OH-Pr^{++}), and Pr^{++} is not formed in the $HPr^+/O_2^{\cdot-}$ reaction. However, in the presence of other oxidants (e.g., $ONOO^-$, hydroxyl radical, or peroxidatic activity), other oxidation products (e.g., Pr^{++} and dimeric products, Pr^{++}-Pr^{++}, HPr^+-HPr^+, HPr^+-Pr^{++}) are formed (Fig. 2). HPLC or UHPLC and LC-MS/MS techniques were used to separate and identify these products [20]. Like the HE-derived radical, the HPr^+-derived radical also does not reduce oxygen to superoxide. The HPr^+ fluorescent probe is suitable for detecting extracellularly generated $O_2^{\cdot-}$ [20, 51].

Table 1 Structures of probes, marker products, and species detected

Probe	Diagnostic product(s)	ROS/RNS species	Detection technique(s)
Hydroethidine (HE) 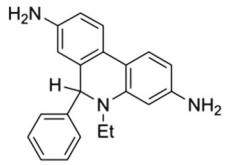	2-Hydroxyethidium (2-OH-E$^+$) 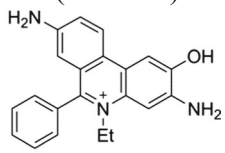	$O_2^{\cdot}$ -specific product	• HPLC with fluorescence detection • LC-MS • Fluorimetry of the complex of 2-OH-E$^+$ with DNA
	2-Chloroethidium (2-Cl-E$^+$) 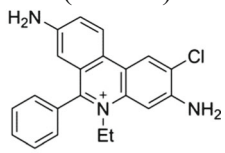	HOCl-specific product	• LC-MS
Hydropropidine (HPr$^+$) 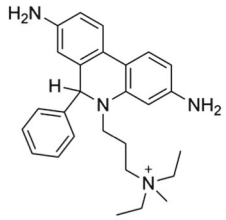	2-Hydroxypropidium (2-OH-Pr^{++}) 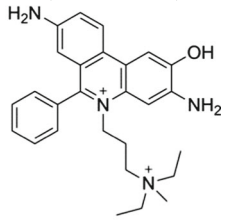	$O_2^{\cdot}$ -specific product	• HPLC with fluorescence detection • LC-MS • Fluorimetry of the complex of 2-OH-Pr^{++} with DNA
Coumarin boronic acid (CBA) 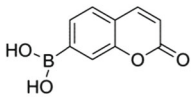	7-Hydroxycoumarin (COH) 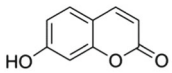	H_2O_2 (catalase-sensitive) $ONOO^-$ (catalase-insensitive) HOCl (catalase-sensitive, MPO inhibitor-sensitive)	• HPLC with fluorescence detection • LC-MS • Fluorimetry
Amplex Red 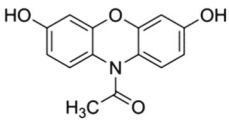	Resorufin 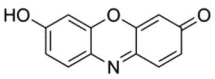	H_2O_2 (HRP-dependent, catalase-sensitive)	• HPLC with fluorescence detection • Fluorimetry
ortho-MitoPhB(OH)$_2$ 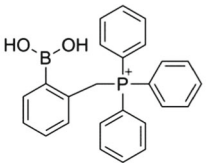	*cyclo-o*-MitoPh 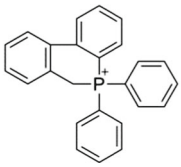	$ONOO^-$-specific product	• LC-MS

Probes for Hydrogen Peroxide Detection

Boronates react with H_2O_2 stoichiometrically to form the corresponding hydroxyl derivative ([32, 49]; Fig. 3a). However, this reaction is very slow (rate constant of ca. 1 $M^{-1}s^{-1}$); therefore, in a cellular milieu, it is unlikely that a boronate probe is the preferred target for H_2O_2. In addition, other oxidants including $ONOO^-$ and HOCl react with boronates at rates higher than does H_2O_2 (with the rate constants in the range of 10^3–10^6 $M^{-1}s^{-1}$, Fig. 3a), and therefore, boronate probes are not suitable for detecting H_2O_2 in cells or tissues under conditions generating $ONOO^-$ or HOCl [32, 52, 53]. Under extracellular conditions, we monitored H_2O_2 formation using the coumarin boronate acid (CBA) probe (Fig. 3b; Table 1) with and without the catalase enzyme [51]. Peroxynitrite-mediated oxidation of boronates is not sensitive to catalase [32, 48, 49]. In addition, it will be necessary to rule out myeloperoxidase/H_2O_2/Cl^--dependent oxidation of boronate via HOCl, as catalase could also inhibit this reaction.

The Amplex Red assay is widely used for H_2O_2 detection and quantification because of its high sensitivity. This assay is based on a horseradish peroxidase (HRP)/H_2O_2-dependent oxidation of Amplex Red probe to resorufin. Resorufin has a high extinction coefficient in the visible absorption region and can be conveniently monitored to measure extracellularly generated H_2O_2 (Table 1). Interference from photosensitized oxidation of Amplex Red by the analyzing (excitation) light, as well as other, H_2O_2-independent pathways of conversion of Amplex Red to resorufin, should be considered [23, 43]. Due to the requirement of HRP catalysis, the use of Amplex Red probe is limited to cell-free and extracellularly released H_2O_2.

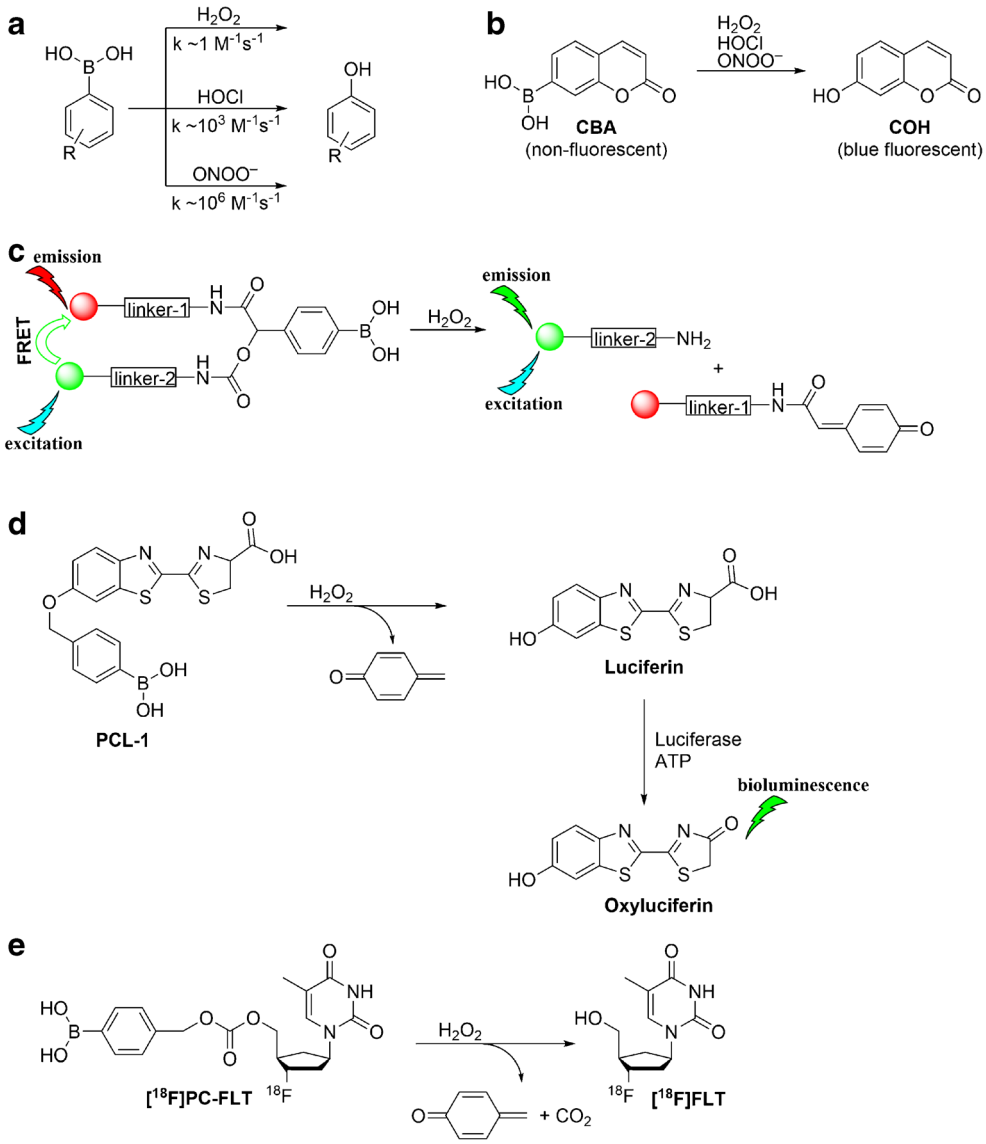

Fig. 3 Oxidation of boronate probes by hydrogen peroxide, hypochlorite, and peroxynitrite. **a** Comparison of the rate constants for different oxidants. **b**–**e** Examples of the boronate-based probes for in vitro and in vivo applications

Probes for Peroxynitrite Detection

Although over the last 5 years, an array of fluorogenic probes for the detection of $ONOO^-$ has been reported (e.g., [16, 26, 36, 39, 44]), boronate-based probes seem to be best suited for that purpose. We have previously shown that boronate-based compounds react with peroxynitrite either added as a bolus or formed in situ from simultaneous generation of $^{\cdot}NO$ and $O_2^{\cdot-}$ nearly six orders of magnitude (10^6-fold) faster than H_2O_2 [32, 48]. The major product of this reaction is the corresponding hydroxyl derivative (phenol or alcohol), and the minor product (10 %) was from an intermediate radical [32, 33, 49, 52]. Indeed, the minor pathway led to nitrated benzene derivatives as the most diagnostic product [32, 33, 52]. Formation of minor products from the CBA probe (e.g., 7-nitrocoumarin, CNO_2, Fig. 4a) allowed us to unequivocally demonstrate the formation of $ONOO^-$ during the reaction of HNO with O_2 [34]. Recently, we have characterized a new cyclic product, formed during the reaction with *ortho*-substituted boronate (*o*-MitoPhB$(OH)_2$) via the phenyl radical addition to the phenyl ring of the triphenylphosphonium moiety (Fig. 4b, Table 1; [53]). By choosing the appropriate boronate, its reaction with $ONOO^-$ can be monitored in real time using fluorescence or bioluminescence techniques [49, 50]. Figure 3b shows the reaction between $ONOO^-$ and coumarin boronate. Whereas coumarin boronate CBA is not fluorescent, the product (7-hydroxycoumarin [COH]) is fluorescent, and $ONOO^-$ can be monitored conveniently by monitoring COH by fluorescence in the presence of added catalase to exclude the minor reaction with H_2O_2 ([48, 50]; Table 1).

By modifying the chemical structure, the fluorescence parameters can be altered. If the product absorbs in the red region, the applicability to in vivo situation is feasible. For in vivo applications, because of the poor tissue penetration of short-wavelength light, it is important to have boronates that yield products absorbing in the red or infrared regions [7, 40].

Mitochondrial Superoxide Detection: Problems with Mito-SOX

Recently, using a mitochondria-targeted hydroethidine probe (Mito-HE or Mito-SOX), superoxide generated in mitochondria was monitored [29]. In every aspect, the reaction chemistry between HE or Mito-SOX with superoxide and other oxidants is identical [46, 47]. For example, Mito-hydroethidine is oxidized by superoxide to form the characteristic 2-hydroxy-Mito-ethidium ([47]; Fig. 2). As with red fluorescence derived from HE oxidation, Mito-SOX/ROS-derived red fluorescence cannot be equated to superoxide detection and measurement [47], and it is essential to identify the product 2-hydroxy-Mito-ethidium (2-OH-Mito-E^+) by HPLC or LC-MS before implicating superoxide involvement [12, 47]. These and other pitfalls of using a Mito-SOX probe to measure mitochondrial $O_2^{\cdot-}$ were elegantly described in a recent review [27]. Thus, nearly all of the studies that used Mito-SOX-red fluorescence as a measure of $O_2^{\cdot-}$ levels need to be repeated and reevaluated with rigorous methodologies using the LC-MS or HPLC techniques [25].

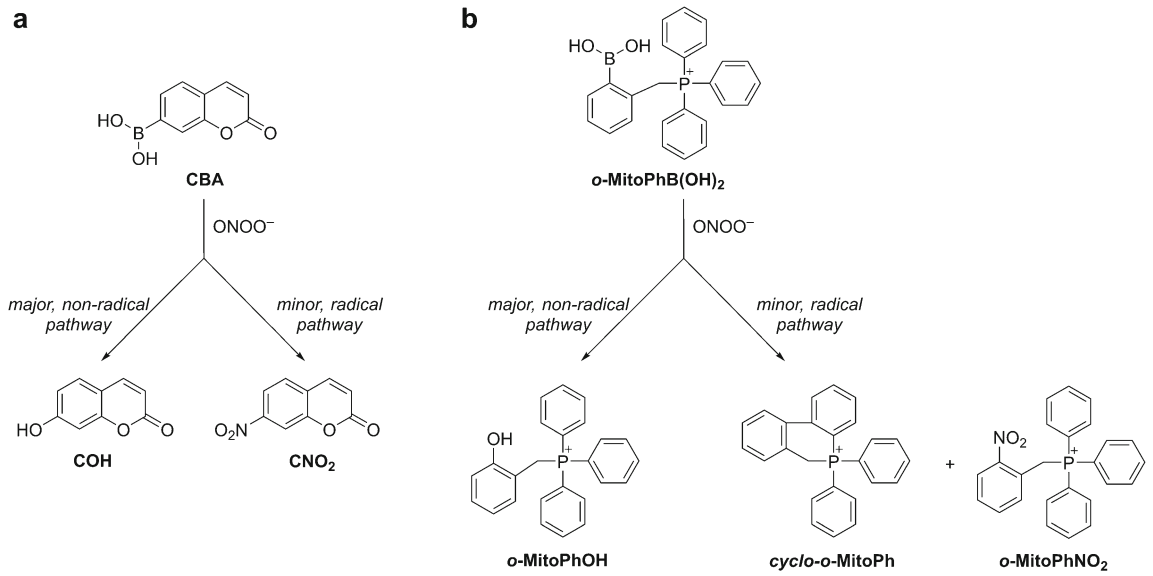

Fig. 4 Chemical structures of the major and minor products formed during the reaction of $ONOO^-$ with **a** CBA and **b** *o*-MitoPhB$(OH)_2$ probes

New Probes Developed in Other Laboratories: Assessment and Reinterpretation of Results

In Vivo Detection of Superoxide: Radiolabeled Probes

Recently, alternate sensitive and noninvasive approaches (e.g., positron emission tomography [PET] and radionucleotide imaging) for detecting superoxide, suitable for in vivo conditions, were developed [1, 6, 35]. These approaches are based on the intracellular trapping of the oxidation products of HE and its analogs. In PET detection, an ^{18}F-labeled HE analog (Fig. 2) ([^{18}F]-HMe) was used as a PET tracer. This is an interesting imaging modality that is easily translatable to humans, as there exist numerous PET probes (e.g., fluorodeoxyglucose [FDG]) that are currently being used in the clinic to track glycolytic metabolism in humans.

Although this imaging modality is very sensitive, the chemistry between an ^{18}F-labeled HMe probe and ROS is the same as that of the unlabeled DHE and ROS (Fig. 2). Superoxide oxidizes [^{18}F]-HMe to [^{18}F]-2-OH-Me$^+$ (Fig. 2). Other one-electron oxidants will oxidize this probe to the corresponding ^{18}F-labeled ethidium analog and ^{18}F-labeled dimeric oxidation products (Fig. 2). All products having the ^{18}F tracer and trapped intracellularly will be imaged, and there is no way to distinguish between the superoxide-derived product and other nonspecific one-electron oxidation products. In essence, all of the limitations that we have previously described for fluorescence-based imaging are applicable to PET imaging as well [12, 47]. In addition, as with the unlabeled DHE that undergoes oxidation in the presence of heme (or hemoglobin), this PET tracer is also subject to nonspecific heme-catalyzed oxidation [47]. Any claims for noninvasive imaging of superoxide using this probe (in vivo or in vitro) should be reexamined. However, this probe may be used to investigate oxidative stress or oxidants formed in diseased and normal brains using PET imaging because of the likelihood of the ^{18}F-labeled analog of DHE, and not the positively charged ethidium analog, crossing the blood–brain barrier [6].

Another radiolabeled HE analog (^{3}H-hydromethidine, [C^{3}H$_3$]-HMe) (Fig. 2) containing the radiotracer tritium was recently developed to probe oxyradical formation in the brain [35]. Again, the radical chemistry of ^{3}H-hydromethidine should be very similar to that of HE. Superoxide oxidizes [C^{3}H$_3$]-HMe to [C^{3}H$_3$]-2-OH-Me$^+$ and nonspecific one-electron oxidation products include [C^{3}H$_3$]-Me$^+$ and ^{3}H-labeled dimers of hydromethidine (Fig. 2). A claim that $O_2^{\cdot-}$ reacts with ^{3}H-hydromethidine to form ^{3}H-methidium rather than a hydroxylated cation has not been substantiated. The authors cite a previous publication by Hall et al. [11] wherein $O_2^{\cdot-}$ reacts with hydroethidine under in vivo conditions to form ethidium and not 2-hydroxyethidium. That $O_2^{\cdot-}$ reacts with hydroethidine to form ethidium under low oxygen tension (but not at normal oxygen tension) was recently challenged by us [21]. We showed that irrespective of the superoxide flux, the major product of HE/$O_2^{\cdot-}$ reaction is 2-hydroxyethidium and not ethidium [21]. Simply measuring the extent of radioactivity in tissues is not sufficient for determining the identity of ROS; the products must be separated using the HPLC-radiolabeled detection method and the retention time compared with that of the appropriate standard. Despite the fact that the use of ^{3}H-hydromethidine radiotracer is unlikely to yield definite information regarding the nature of an oxidant(s) formed in tissues or cells, the ability of the parent tracer to cross the blood–brain barrier is an advantage. The contribution of oxidative stress in the brain under pathological conditions can be qualitatively assessed.

In Vivo Targeting of Hydrogen Peroxide: Cell-Penetrating Peptides

Recently, in vivo detection of hydrogen peroxide was reported using a newly developed probe consisting of a polycationic cell-penetrating peptide and a polyanionic fragment connected through a boronate linker [37]. Fluorescent labeling of both of its peptide domains resulted in the fluorescence resonance energy transfer (FRET) signal (Fig. 3c). Reaction with H_2O_2 caused a disruption of FRET which was used to measure H_2O_2. Using the 40-fold ratio change in FRET, H_2O_2 generated by activated macrophages and neutrophils in a lipopolysaccharide (LPS) mouse model of inflammation was monitored [37]. However, several caveats with the use of this probe were not discussed in that study [37]. Boronates react very slowly with H_2O_2; in an intracellular milieu, this reaction probability is very low. We reported that $ONOO^-$ reacts with boronates at least a million times faster than with H_2O_2 [32]. As discussed earlier, reports indicate that $ONOO^-$ is generated during LPS treatment. Thus, additional experiments with NOS and/or Nox and MPO inhibitors (to rule out contribution from HOCl) are necessary for proper interpretation of the data reported in this study [37] as well as in another study using a lysosome-targeted boronate-based probe [13].

Bioluminescence and PET Imaging of ROS In Vivo

One of the most convenient modes of in vivo animal imaging is based on bioluminescence. Thus, a new probe has been synthesized, peroxy-caged luciferin-1 (PCL-1), which upon reaction with ROS/RNS forms luciferin in situ that is rapidly oxidized in luciferase-transfected cells generating green bioluminescence [31, 38]. This reaction uses adenosine triphosphate (ATP) as a cofactor (Fig. 3d).

A PET probe for detecting H_2O_2 was recently developed [4]. This ROS-specific PET agent is a thymidine analog, peroxy-caged-[^{18}F]fluorodeoxy thymidine [^{18}F]PC-FLT that is transported rapidly into cells via the nucleoside transporter. Unlike thymidine, [^{18}F]PC-FLT is not phosphorylated by

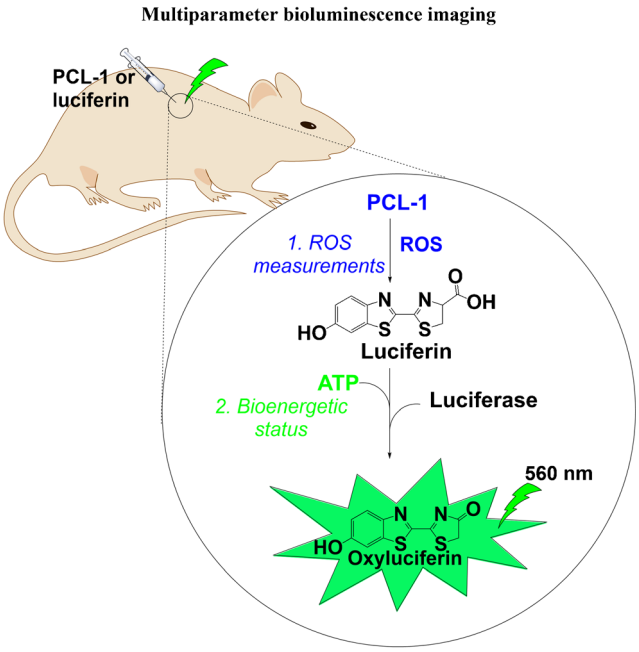

Fig. 5 Proposed approach for luciferin-based bioluminescence imaging of ROS and bioenergetic status in vivo

thymidine kinase and does not accumulate inside the cell [4]. Upon reaction with H_2O_2, PC-FLT-1 generated [^{18}F]FLT in situ (Fig. 3e) that is phosphorylated, trapped intracellularly, and imaged by PET.

As discussed for other boronate probes [31, 32, 49], the PCL-1 and PC-FLT probes react with H_2O_2 rather slowly to be considered as effective H_2O_2 detectors in cells. Under conditions where $ONOO^-$ and/or HOCl are generated, these probes will undoubtedly react with these species as opposed to H_2O_2.

Conclusion and Future Perspectives

With the advent of new and sensitive probes with relatively lower toxicity and better spatial resolution developed primarily in Chang's laboratory [17], we are in a position to perform relevant preclinical imaging that can be translated to the clinical setting [4]. [^{18}F]FLT is used in the clinic, and boronates have been administered to cancer patients for many years. Thus, it is conceivable that the peroxy-caged probe, [^{18}F]PC-FLT, containing the boronate moiety will be tested in the clinic for imaging RNS. Equally significant and promising are the boronate-based bioluminescence probes. For example, the newly synthesized peroxy-caged luciferin-1 (PCL-1), upon reaction with ROS/RNS, forms luciferin in situ that is rapidly oxidized in luciferase-transfected cells generating green bioluminescence [31, 38]. This reaction uses ATP as a cofactor. As with other boronates, PCL-1 reacts with $ONOO^-$ nearly a million times faster than with H_2O_2 and thus could be used to image $ONOO^-$ formation in an inflammatory microenvironment in various toxicology models. With the proper experimental setup, we should be able to monitor the effects of pesticides on multiple cellular parameters including H_2O_2/$ONOO^-$ generation and, for example, cellular bioenergetic status (ATP level), with a single detection modality (e.g., bioluminescence), as exemplified in Fig. 5.

Acknowledgments This work was supported by funds received from the National Institutes of Health (R01 HL063119 and R01 HL073056).

Compliance with Ethical Standards

Conflict of Interest The authors declare that they have no conflicts of interest.

Human and Animal Rights and Informed Consent This article does not contain any studies with human or animal subjects performed by any of the authors.

References

1. Abe K et al. In vivo imaging of reactive oxygen species in mouse brain by using [3H]hydromethidine as a potential radical trapping radiotracer. J Cereb Blood Flow Metab. 2014;34:1907–13.
2. Al Ghouleh I et al. Oxidases and peroxidases in cardiovascular and lung disease: new concepts in reactive oxygen species signaling. Free Radic Biol Med. 2011;51:1271–88.
3. Beckman JS et al. Apparent hydroxyl radical production by peroxynitrite: implications for endothelial injury from nitric oxide and superoxide. Proc Natl Acad Sci U S A. 1990;87:1620–4.
4. Carroll V et al. A boronate-caged [^{18}F]FLT probe for hydrogen peroxide detection using positron emission tomography. J Am Chem Soc. 2014;136:14742–5.
5. Carter WO, Narayanan PK, Robinson JP. Intracellular hydrogen peroxide and superoxide anion detection in endothelial cells. J Leukoc Biol. 1994;55:253–8.
6. Chu W et al. Development of a PET radiotracer for non-invasive imaging of the reactive oxygen species, superoxide, in vivo. Org Biomol Chem. 2014;12:4421–31.
7. Dickinson B, Huynh C, Chang CJ. A palette of fluorescent probes with varying emission colors for imaging hydrogen peroxide signaling in living cells. J Am Chem Soc. 2010;132:5906–15.
8. Dranka BP et al. Diapocynin prevents early Parkinson's disease symptoms in the leucine-rich repeat kinase 2 (LRRK2R^{1441}G) transgenic mouse. Neurosci Lett. 2013;549:57–62.
9. Finkle T. Signal transduction by reactive oxygen species. J Cell Biol. 2011;194:7–15.
10. Ghassan J et al. Assessment of myeloperoxidase activity by the conversion of hydroethidine to 2-chloroethidium. J Biol Chem. 2014;289:5580–95.
11. Hall DJ et al. Dynamic optical imaging of metabolic and NADPH oxidase-derived superoxide in live mouse brain using fluorescence lifetime unmixing. J Cereb Blood Flow Metab. 2012;32:23–32.
12. Kalyanaraman B et al. HPLC-based monitoring of products formed from hydroethidine-based fluorogenic probes—the ultimate approach for intra- and extracellular superoxide detection. Biochim Biophys Acta. 2014;1840:739–44.

13. Kim D et al. Visualization of endogenous and exogenous hydrogen peroxide using a lysosome-targetable fluorescent probe. Sci Rep. 2015;5:8488.
14. Lambeth JD. NOX enzymes and the biology of reactive oxygen. Nat Rev Immunol. 2004;4:181–9.
15. Leto TL. Targeting and regulation of reactive oxygen species generation by Nox family NADPH oxidases. Antioxid Redox Signal. 2009;11:2607–19.
16. Li X et al. Visualizing peroxynitrite fluxes in endothelial cells reveals the dynamic progression of brain vascular injury. J Am Chem Soc. 2015;137:12296–303.
17. Lippert AR et al. Boronate oxidation as a bioorthogonal reaction approach for studying the chemistry of hydrogen peroxide in living systems. Acc Chem Res. 2011;44(9):793–804.
18. Mangum LC et al. Organochlorine insecticides induce NADPH oxidase-dependent reactive oxygen species in human monocytic cells via phospholipase A2/arachidonic acid. Chem Res Toxicol. 2015;28:570–84.
19. Mao H, Liu B. Synergistic microglia reactive oxygen species generation induced by pesticides lindane and dieldrin. Oncogene. 2008;19:1317–20.
20. Michalski R et al. Hydropropidine: a novel, cell-impermeant fluorogenic probe for detecting extracellular superoxide. Free Radic Biol Med. 2013;54:135–47.
21. Michalski R et al. On the use of fluorescence lifetime imaging and dihydroethidium to detect superoxide in intact animals and ex vivo tissues: a reassessment. Free Radic Biol Med. 2014;67:278–84.
22. Min JY et al. Potential role for organochlorine pesticides in the prevalence of peripheral arterial diseases in obese persons: results from the National Health and Nutrition Examination Survey 1999–2004. Atherosclerosis. 2011;218:200–6.
23. Miwa S et al. Carboxylesterase converts Amplex red to resorufin: implications for mitochondrial H2O2 release assays. Free Radic Biol Med. 2016;90:173–83.
24. Nisimoto Y et al. Nox4: a hydrogen peroxide-generating oxygen sensor. Biochemistry. 2014;53:5111–20.
25. Papa L et al. SOD2 to SOD1 switch in breast cancer. J Biol Chem. 2014;289:5412–6.
26. Peng T et al. Molecular imaging of peroxynitrite with HKGreen-4 in live cells and tissues. J Am Chem Soc. 2014;136:11728–34.
27. Polster BM et al. Use of potentiometric fluorophores in the measurement of mitochondrial reactive oxygen species. Methods Enzymol. 2014;547:225–50.
28. Radi R et al. Peroxynitrite oxidation of sulfhydryls. The cytotoxic potential of superoxide and nitric oxide. J Biol Chem. 1991;266:4244–50.
29. Robinson KM et al. Selective fluorescent imaging of superoxide in vivo using ethidium-based probes. Proc Natl Acad Sci U S A. 2006;103:15038–43.
30. Serrandel L et al. NOX4 activity is determined by mRNA levels and reveals a unique pattern of ROS generation. Biochem J. 2007;406:105–14.
31. Sieracki NA et al. Bioluminescent detection of peroxynitrite with a boronic acid-caged luciferin. Free Radic Biol Med. 2013;61:40–50.
32. Sikora A et al. Direct oxidation of boronates by peroxynitrite: mechanism and implications in fluorescence imaging of peroxynitrite. Free Radic Biol Med. 2009;47:1401–7.
33. Sikora A et al. Reaction between peroxynitrite and boronates: EPR spin-trapping, HPLC analyses, and quantum mechanical study of the free radical pathway. Chem Res Toxicol. 2011;24:687–97.
34. Smulik R et al. Nitroxyl (HNO) reacts with molecular oxygen and forms peroxynitrite at physiological pH biological implications. J Biol Chem. 2014;289:35570–81.
35. Takai N et al. Imaging of reactive oxygen species using [(3)H]hydromethidine in mice with cisplatin-induced nephrotoxicity. EJNMMI Res. 2015;5:116.
36. Wang B et al. A BODIPY fluorescence probe modulated by selenoxide spirocyclization reaction for peroxynitrite detection and imaging in living cells. Dye Pigment. 2013;96:383–90.
37. Weinstain R et al. In vivo targeting of hydrogen peroxide by activatable cell-penetrating peptides. J Am Chem Soc. 2014;136:874–7.
38. Van de Bittner GC et al. In vivo imaging of hydrogen peroxide production in a murine tumor model with a chemoselective bioluminescent reporter. Proc Natl Acad Sci U S A. 2010;107:21316–21.
39. Xu K et al. A near-infrared reversible fluorescent probe for peroxynitrite and imaging of redox cycles in living cells. Chem Commun. 2011;47:9468–70.
40. Yuan L et al. A unique approach to development of near-infrared fluorescent sensors for in vivo imaging. J Am Chem Soc. 2012;134:13510–23.
41. Zhao H et al. Superoxide reacts with hydroethidine but forms a fluorescent product that is distinctly different from ethidium: potential implications in intracellular fluorescence detection of superoxide. Free Radic Biol Med. 2003;34:1359–68.
42. Zhao H et al. Detection and characterization of the product of hydroethidine and intracellular superoxide by HPLC and limitations of fluorescence. Proc Natl Acad Sci U S A. 2005;102:5727–32.
43. Zhao B, Summers FA, Mason RP. Photooxidation of Amplex Red to resorufin: implications of exposing the Amplex Red assay to light. Free Radic Biol Med. 2012;53:1080–7.
44. Zhou X et al. A ratiometric fluorescent probe based on a coumarin-hemicyanine scaffold for sensitive and selective detection of endogenous peroxynitrite. Biosens Bioelectron. 2015;64:285–91.
45. Zielonka J et al. Detection of 2-hydroxyethidium in cellular systems: a unique marker product of superoxide and hydroethidine. Nat Protoc. 2008;3:8–21.
46. Zielonka J et al. Cytochrome c-mediated oxidation of hydroethidine and mito-hydroethidine in mitochondria: identification of homo- and heterodimers. Free Radic Biol Med. 2008;44:835–46.
47. Zielonka J, Kalyanaraman B. Hydroethidine- and MitoSOX-derived red fluorescence is not a reliable indicator of intracellular superoxide formation: another inconvenient truth. Free Radic Biol Med. 2010;48:983–1001.
48. Zielonka J et al. Peroxynitrite is the major species formed from different flux ratios of co-generated nitric oxide and superoxide: direct reaction with boronate-based fluorescent probe. J Biol Chem. 2010;285:14210–6.
49. Zielonka J et al. Boronate probes as diagnostic tools for real time monitoring of peroxynitrite and hydroperoxides. Chem Res Toxicol. 2012;25:1793–9.
50. Zielonka J et al. Global profiling of reactive oxygen and nitrogen species in biological systems: high-throughput real-time analyses. J Biol Chem. 2012;287:2984–95.
51. Zielonka J et al. High-throughput assays for superoxide and hydrogen peroxide: design of a screening workflow to identify inhibitors of NADPH oxidases. J Biol Chem. 2014;289:16176–89.
52. Zielonka J et al. Detection and differentiation between peroxynitrite and hydroperoxides using mitochondria-targeted arylboronic acid. Methods Mol Biol. 2015;1264:17181.
53. Zielonka J et al. Mitigation of NADPH oxidase 2 activity as a strategy to inhibit peroxynitrite formation. J Biol Chem. 2016;291:7029–44.